NEUROSCIENCE

A cortical-brainstem circuit predicts and governs compulsive alcohol drinking

Cody A. Siciliano[1,2,3]*, Habiba Noamany[1], Chia-Jung Chang[1], Alex R. Brown[1,2,3], Xinhong Chen[1], Daniel Leible[1], Jennifer J. Lee[1], Joyce Wang[1], Amanda N. Vernon[1], Caitlin M. Vander Weele[1], Eyal Y. Kimchi[1], Myriam Heiman[1], Kay M. Tye[1,4]*

What individual differences in neural activity predict the future escalation of alcohol drinking from casual to compulsive? The neurobiological mechanisms that gate the transition from moderate to compulsive drinking remain poorly understood. We longitudinally tracked the development of compulsive drinking across a binge-drinking experience in male mice. Binge drinking unmasked individual differences, revealing latent traits in alcohol consumption and compulsive drinking despite equal prior exposure to alcohol. Distinct neural activity signatures of cortical neurons projecting to the brainstem before binge drinking predicted the ultimate emergence of compulsivity. Mimicry of activity patterns that predicted drinking phenotypes was sufficient to bidirectionally modulate drinking. Our results provide a mechanistic explanation for individual variance in vulnerability to compulsive alcohol drinking.

More than 80% of adults are exposed to alcohol during their lifetime (*1*), yet less than 30% will develop an alcohol use disorder (AUD) (*2*). How exposure to alcohol can produce such disparate outcomes between individuals remains poorly understood.

Compulsive alcohol drinking, defined as continued drinking in the face of a negative consequence (*3*, *4*), is a distinguishing feature of AUDs (*5*). The medial prefrontal cortex (mPFC) is critical in mediating pathological drug-seeking behaviors, including compulsion (*6*–*10*). Both preexisting (*11*–*13*) and alcohol-induced changes in PFC function can contribute to maladaptive behaviors including compulsive drinking (*14*–*17*). Although rodent models have advanced our understanding of drinking behavior (*14*, *18*–*21*), neural correlates are typically assessed at a single end point, after long-term exposure to alcohol, thereby occluding individual differences in compulsion vulnerability as well as the longitudinal nature of its development.

We developed a "binge-induced compulsion task" (BICT) to assess how predisposition interacts with experience to produce compulsive drinking (Fig. 1A). Initially, an auditory conditioned stimulus (CS+) predicted delivery of sucrose until animals reliably responded (see the materials and methods). During pre-binge (days 1 to 3), the CS+ predicted delivery of alcohol alone (15%). On days 4 to 5, increasing concentrations of quinine, a bitter tastant used as a punishment (*3*), were added to the alcohol (alcohol+quinine). During binge drinking (days 6 to 19), animals had unlimited access to water and alcohol for 0, 2, or 4 hours

[1]The Picower Institute for Learning and Memory, Department of Brain and Cognitive Sciences, Massachusetts Institute of Technology, Cambridge, MA 02139, USA. [2]Department of Pharmacology, Vanderbilt University School of Medicine, Nashville, TN 37232, USA. [3]Vanderbilt Center for Addiction Research, Vanderbilt University School of Medicine, Nashville, TN 37232, USA. [4]The Salk Institute for Biological Studies, La Jolla, CA 92037, USA.
*Corresponding author. Email: tye@salk.edu (K.M.T.); cody.siciliano@vanderbilt.edu (C.A.S.)

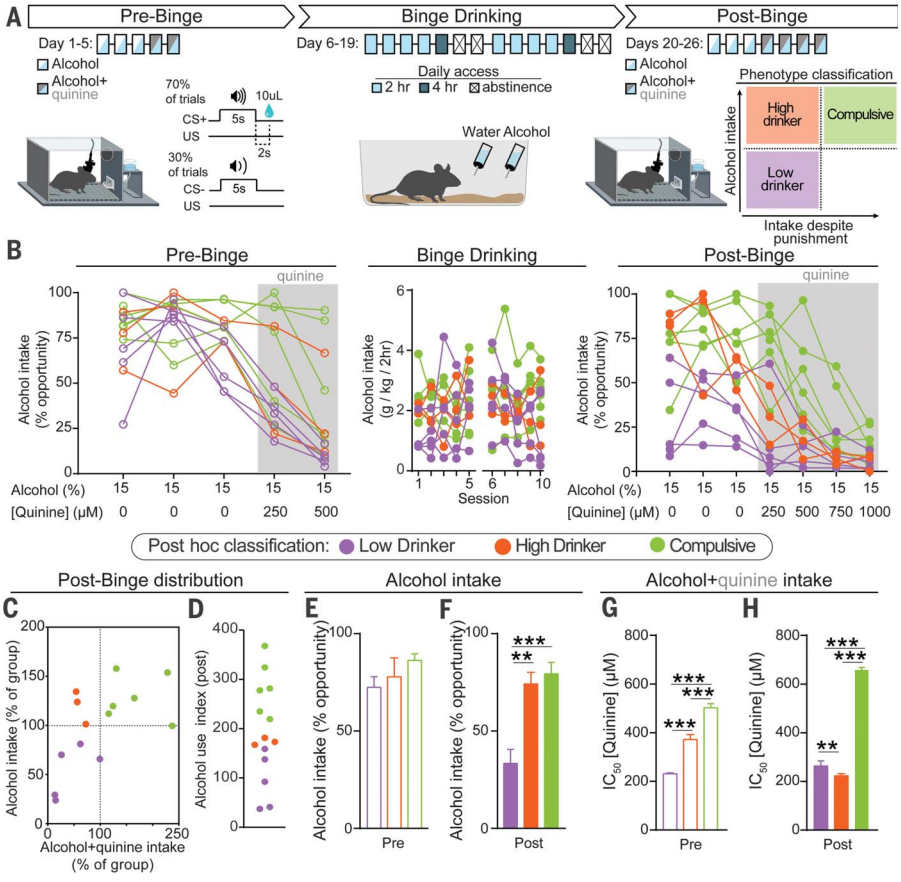

Fig. 1. Binge-induced compulsion task (BICT) for tracking the emergence of individual differences in compulsive alcohol drinking. (**A**) Schematic of the BICT. (**B**) Individual animals' alcohol consumption. (**C**) Normalized distributions of alcohol and alcohol+quinine consumption during the post-binge conditioning phase plotted to classify each animal's alcohol-drinking phenotype, which was applied post hoc to the dataset. (**D**) Alcohol use index. (**E**) Average performance across the pre-binge alcohol-only sessions (days 1 to 3) did not differ between groups [one-way analysis of variance (ANOVA), $F_{(2,11)} = 1.922$, $p = 0.19$]. (**F**) During post-binge conditioning sessions, high drinkers and compulsive animals consumed more alcohol (one-way ANOVA, $F_{(2,11)} = 15.41$, $p = 0.0006$). (**G**) Concentration required to produce an IC_{50} calculated from pre-binge conditioning data (one-way ANOVA, $F_{(2,11)} = 430.3$, $p < 0.0001$). (**H**) After binge drinking, compulsive animals exhibited robust punishment-resistant alcohol intake compared with both low and high drinkers (one-way ANOVA, $F_{(2,11)} = 1298.0$, $p < 0.0001$). All post hoc comparisons used Tukey's test: $^{**}p < 0.01$; $^{***}p < 0.001$. Error bars indicate ± SEM.

per day, producing high, "binge-like" levels of alcohol intake (*22*). During post-binge (days 20 to 26), animals returned to the pre-binge conditioning context, in which alcohol alone was presented for 3 days, followed by alcohol +quinine for the next 4 days (Fig. 1A). Intake volumes correlated with blood alcohol content (fig. S1).

The BICT allows for longitudinal assessment of two behavioral outcomes associated with diagnostic criteria for AUDs (*5*): alcohol consumption and continued consumption despite negative outcomes. After binge drinking, there were wide individual differences in drinking, both in the absence and presence of quinine (Fig. 1B). Three phenotypic classifications were made based on post-binge behavior: mice that displayed low alcohol intake with and without punishment were termed "low drinkers"; mice that showed high levels of alcohol drinking but were sensitive to punishment were termed "high drinkers"; mice with high levels of drinking that persisted with punishment were termed "compulsive" (Fig. 1C). Values from the alcohol-only and alcohol +quinine distributions were summed to create an "alcohol use index" for each animal (Fig. 1D).

Each animal was classified on the basis of its behavior during post-binge and designation was retroactively applied. Mice that were eventually divided into the three subgroups showed no detectable differences in unadulterated alcohol intake before binge drinking (Fig. 1E). After binge drinking, low drinkers' intake decreased, even in the absence of punishment (Fig. 1F and fig. S2D). Before binge drinking, compulsive animals showed greater resistance to punishment than both low and high drinkers, as measured by the concentration of quinine required to produce a half-maximal effect on alcohol consumption [half-maximal inhibitory concentration (IC_{50}); Fig. 1G and fig. S2E]. After binge drinking, this phenotype was exacerbated as compulsive animals showed a robust insensitivity to punishment (Fig. 1H and fig. S2F). Longitudinal examination highlighted a substantial divergence among groups when punishment was present: high drinkers showed increased sensitivity to quinine's effects on alcohol intake after binge drinking, whereas compulsive animals showed decreased sensitivity (fig. S2G). There were no group differences in alcohol consumption during binge drinking (fig. S2H).

To determine whether phenotypic differences in drinking reflected responses to punishment in general and were not driven by quinine-specific effects, we punished alcohol consumption with foot shock (fig. S3A). Phenotypic drinking behavior was

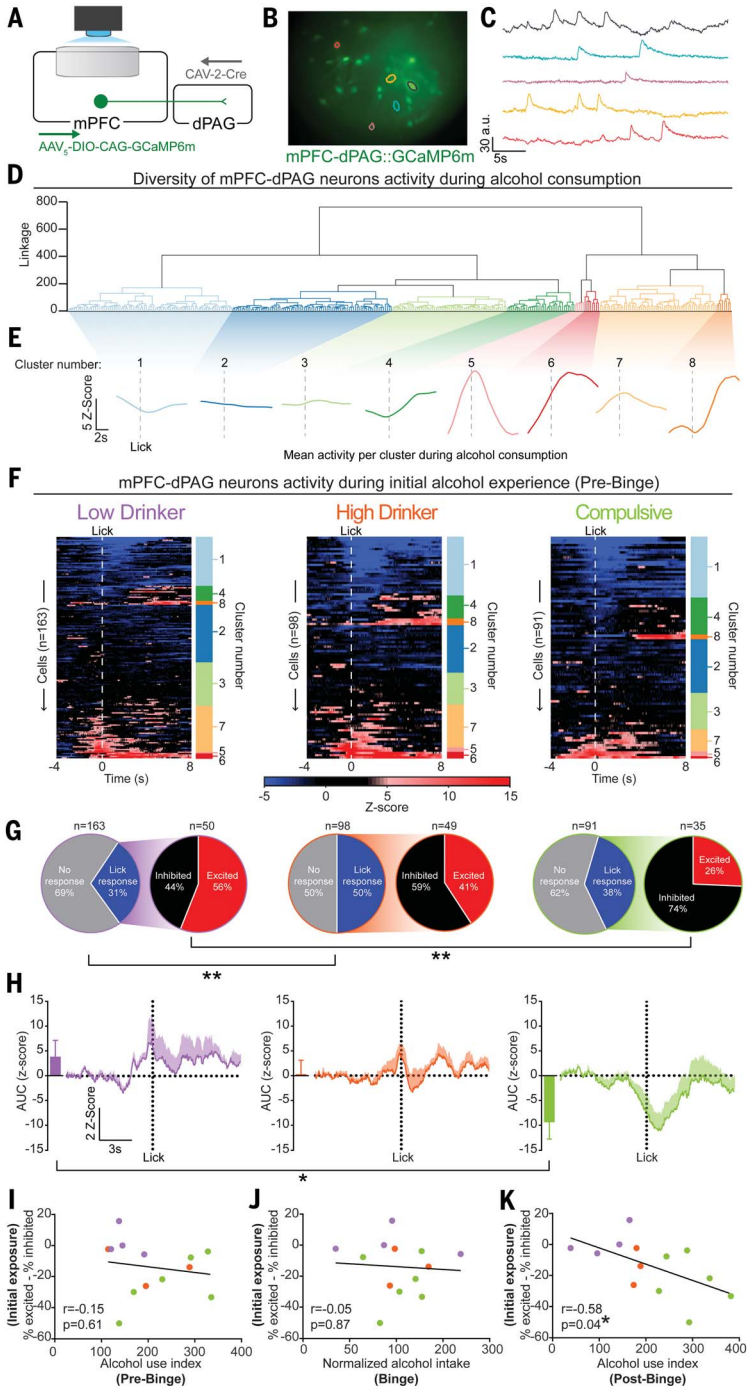

Fig. 2. Activity in mPFC-dPAG neurons during initial experience with alcohol is a vulnerability marker for future alcohol abuse-like behaviors. (**A**) Monitoring mPFC-dPAG activity using in vivo calcium imaging. (**B** and **C**) Field of view (B) and activity traces (C) from example cells. (**D**) Agglomerative hierarchical clustering of calcium activity traces during the first session of pre-binge (n = 13 animals, 352 cells). (**E**) Smoothed and averaged peristimulus time histograms per cluster. (**F**) Cluster designations are to the right of each neuron's heatmap of z-scored trial-averaged activity. (**G**) Differences in distributions of activity during alcohol consumption (Fisher's exact test: $^{**}p < 0.01$). (**H**) Population activity from lick-responsive neurons. Inset: Area under the curve (AUC) for each trace (one-way ANOVA, $F_{(2,10)} = 4.531$, $^{*}p = 0.039$; Tukey's post hoc test, $^{*}p < 0.05$). (**I** to **K**) Balance of excitatory–inhibitory activity during alcohol consumption in the first pre-binge session plotted against each animal's alcohol use index. No correlation between the excitation–inhibition balance during initial exposure and alcohol use index from pre-binge data (I) or from binge drinking (J). (K) Increased inhibitory activity during alcohol consumption during initial exposure predicted heightened pathological-like drinking behaviors during post-binge. Error bars indicate ± SEM.

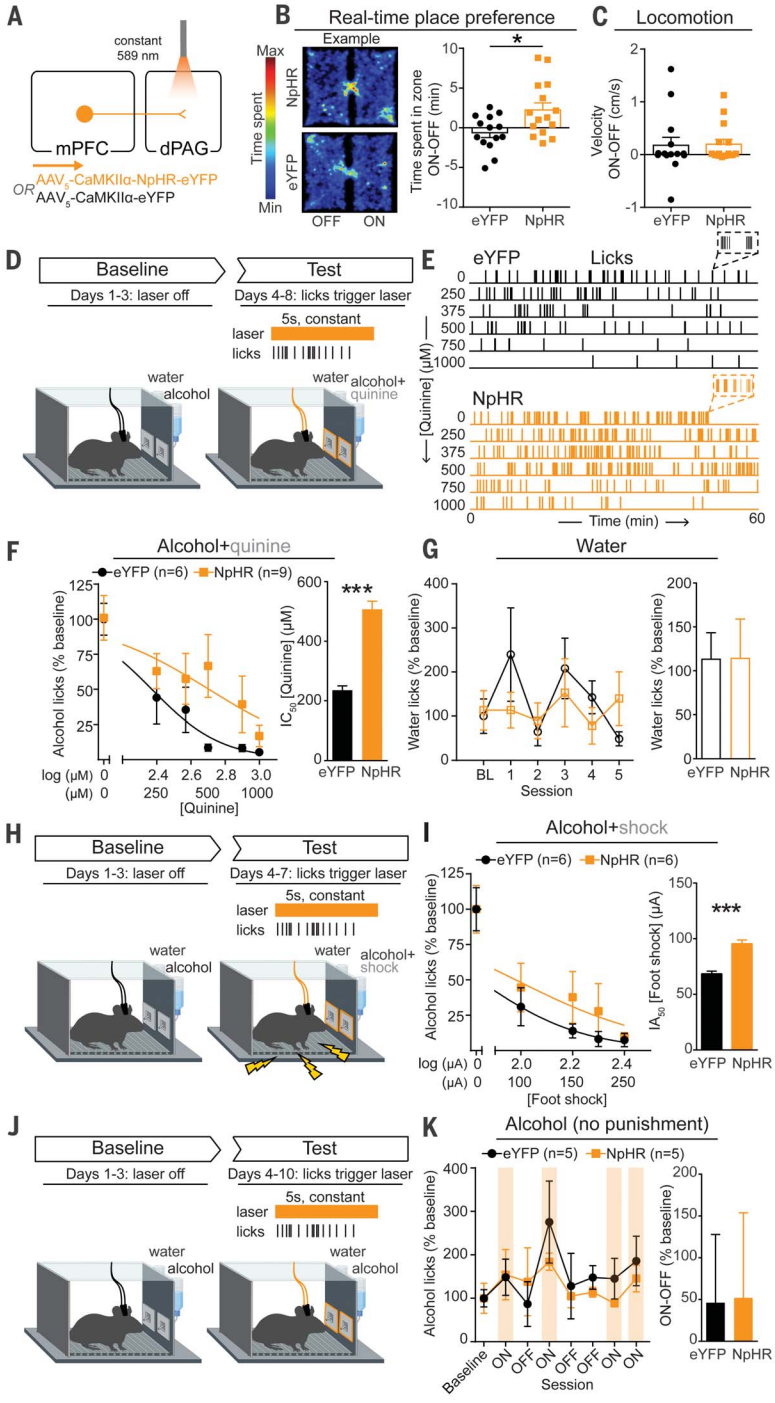

Fig. 3. Inhibition of mPFC-dPAG neurons drives compulsive drinking but does not alter drinking in the absence of punishment. (**A**) Strategy to inhibit mPFC terminals in the dPAG. (**B**) Inhibition of mPFC terminals in the dPAG was preferred in a real-time place preference task (unpaired *t* test, $t_{(27)}$ = 2.647, **p* = 0.013). (**C**) Photoinhibition did not alter locomotion (unpaired *t* test, $t_{(27)}$ = 0.1191, *p* = 0.91). (**D**) On test days, water or alcohol spout contacts triggered a photoinhibition period. During the test, the quinine concentration was increased across days (alcohol bottle only). (**E**) Example alcohol lick event records. (**F**) The concentration of quinine required to decrease alcohol spout licking to 50% of baseline (IC_{50}) was greater in NpHR animals (unpaired *t* test, $t_{(13)}$ =22.05, ****p* < 0.0001). (**G**) No difference in licking for water between groups (unpaired *t* test, $t_{(13)}$ = 0.016, *p* = 0.99). (**H**) Alcohol drinking punished with foot shock. (**I**) Foot-shock amplitude required to attenuate alcohol spout licks by 50% of baseline [half-maximal inhibitory amplitude (IA_{50})] was increased in NpHR animals (unpaired *t* test, $t_{(10)}$ = 6.498, ****p* < 0.0001). (**J**) Alcohol drinking in the absence of punishment. (**K**) Photoinhibition did not alter licking for alcohol in the absence of punishment (unpaired *t* test, $t_{(8)}$ = 0.045, *p* = 0.97). Error bars indicate ± SEM.

retained, demonstrating that these behavioral traits are reproducible and generalizable (fig S3, B and C).

We reasoned that mPFC circuits involved in "top-down" control of avoidance behavior may underlie susceptibility to developing compulsive drinking behaviors. The periaqueductal gray (PAG) is involved in responding to aversive events (*23*–*27*), as well as negative affective states and hyperalgesia during alcohol withdrawal (*28*, *29*). mPFC neurons projecting to dorsal PAG (mPFC-dPAG) encode aversive events (*24*). We hypothesized that functional deficits in mPFC-dPAG neurons could disrupt aversive processing to drive compulsive drinking.

We used cellular-resolution calcium imaging (*30*) to visualize the activity of mPFC-dPAG neurons during the BICT (Fig. 2). An anterogradely traveling virus allowing for cre-dependent expression of GCaMP6m was injected in the mPFC and a retrogradely traveling virus carrying cre-recombinase was injected into the dPAG (Fig. 2A). A gradient-refractive index lens (fig. S4) and a head-mounted microendoscope allowed observation of calcium dynamics. An example field of view illustrates neurons imaged during the BICT (Fig. 2B) and extracted activity traces (Fig. 2C). Hierarchical clustering performed on activity from 352 neurons aligned around initiation of alcohol consumption during the first pre-binge session revealed eight distinct clusters (Fig. 2, D and E).

Although there was no difference between groups in alcohol intake during the "alcohol-only" sessions throughout pre-binge, dynamics of mPFC-dPAG neurons during alcohol consumption differed between the phenotypic groups (Fig. 2F). During the initial alcohol experience (day 1), more mPFC-dPAG neurons exhibited inhibitory responses for compulsive animals than for low drinkers (Fig. 2G). mPFC-dPAG neurons displayed more excitatory activity in low drinkers than in compulsive animals during alcohol consumption (Fig. 2H). A small proportion of mPFC-dPAG neurons displayed responses to the alcohol-predictive cue (CS+) (fig. S5).

Although there were no detectable differences among groups in *behavioral* performance during initial alcohol exposure (Fig. 1, B and E), the *neural* response during initial exposure predicted the future development of compulsive drinking (Fig. 2, F to H). The proportion of excitatory to inhibitory responses of individual mPFC-dPAG neurons for each animal did not correlate with behavior during pre-binge (Fig. 2I) or binge drinking (Fig. 2J), but *did* correlate with post-binge behavior >2 weeks after the neural recordings during initial exposure were collected (Fig. 2K). A support-vector machine

decoded future behavioral selection of drinking (go) versus not drinking (no go) based on the activity of mPFC-dPAG neurons during consumption of alcohol on the previous trial (fig. S6). This supports the notion that this circuit plays a key role in triggering the transition from moderate to compulsive drinking.

To test whether mimicking endogenous activity could alter behavior, we bilaterally expressed halorhodopsin (NpHR) in mPFC neurons and implanted bilateral optic fibers over the dPAG (Fig. 3A and fig. S7). In a real-time place preference assay, NpHR mice displayed modest preference for the photoinhibition-paired side of the chamber compared with fluorophore [enhanced yellow fluorescent protein (eYFP)]-expressing control mice (Fig. 3B). Photoinhibition did not produce any detectable changes in locomotion (Fig. 3C) or anxiety-related behavior (fig. S8, A to F).

Animals were given concurrent access to alcohol and water for three sessions to establish a baseline level of alcohol intake (Fig. 3D). On day 4, quinine was added to the alcohol bottle only, and the quinine concentration was increased across sessions to assess alcohol intake in the face of punishment (Fig. 3E). During quinine sessions, contacts on water or alcohol lickometers triggered photoinhibition, intended to mimic the inhibitory activity observed in compulsive animals during alcohol licking (Fig. 2H). Photoinhibition concomitant with licking for the alcohol+quinine solution was sufficient to induce a rightward shift in the quinine concentration response curve, resulting in a greater than twofold increase in the IC_{50} of quinine compared with eYFP controls (Fig. 3F) without affecting water consumption (Fig. 3G). When alcohol spout contacts were punished with foot shock (Fig. 3H), photoinhibition again promoted compulsive drinking (Fig. 3I and fig. S9, A and B).

To determine whether photoinhibition of mPFC-dPAG activity drives compulsive drinking by increased reinforcing effects of alcohol or decreased sensitivity to punishment, we measured each component in isolation. Photoinhibition did not change alcohol consumption in the absence of punishment (Fig. 3, J and K, and fig. S9, C and D). To determine whether photoinhibition altered responses to noxious stimuli in the absence of reward, we photoinhibited mPFC-dPAG synapses while animals' tails were immersed in 50°C water and found that photoinhibition slowed latency to withdraw (fig. S8, J to L). Photoinhibition did not support intracranial self-stimulation (fig. S8, G to I) and did not alter extinction of operant alcohol self-administration (fig. S10).

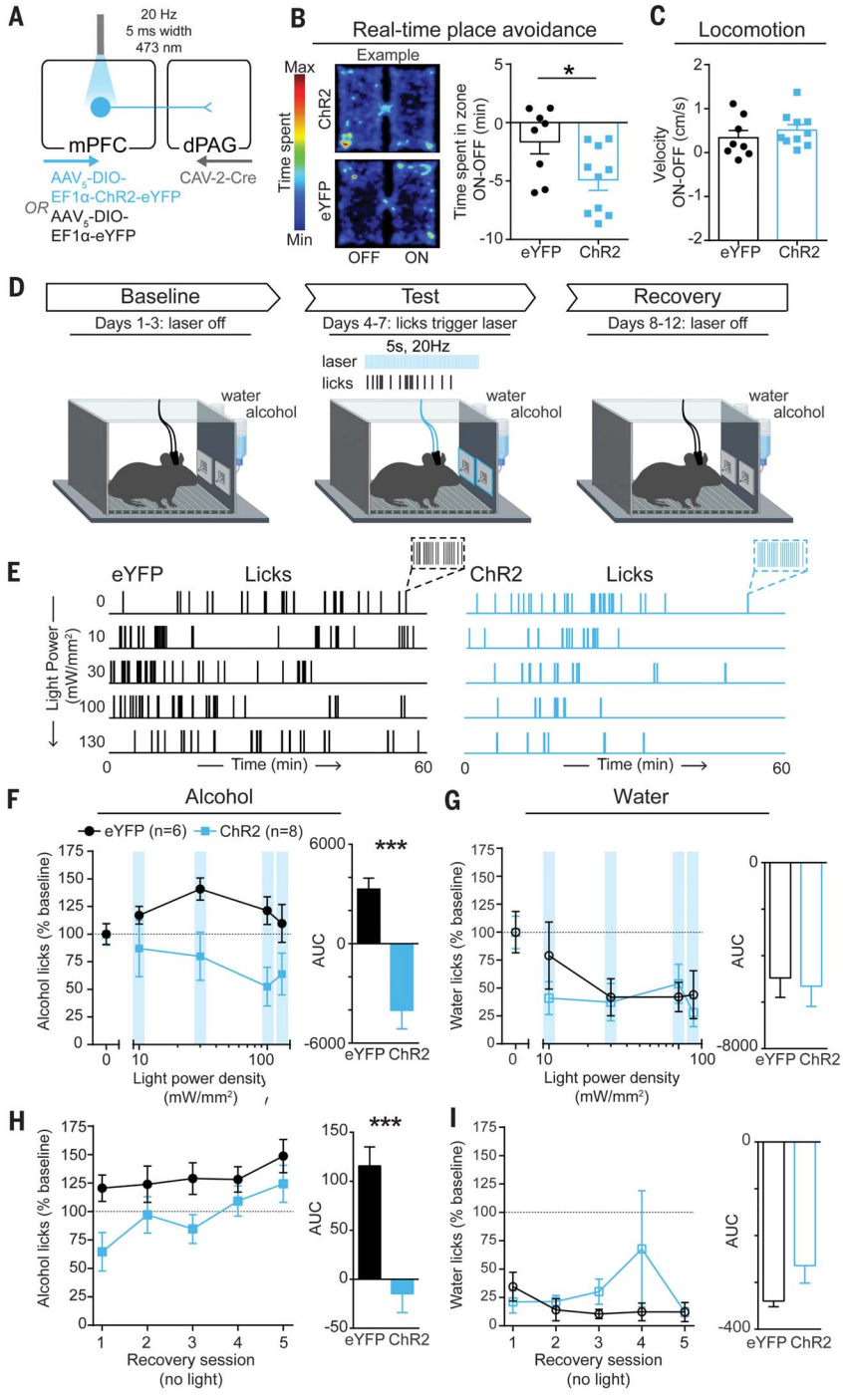

Fig. 4. Activation of mPFC-dPAG neurons mimics the effects of punishment on alcohol consumption. (**A**) Strategy to activate mPFC-dPAG neurons. (**B**) A 20-Hz photostimulation of mPFC-dPAG neurons was avoided in a real-time place avoidance task (unpaired *t* test, $t_{(16)} = 2.356$, **p* = 0.032). (**C**) Photostimulation did not alter locomotion (unpaired *t* test, $t_{(16)} = 0.884$, $p = 0.39$). (**D**) During test days, water or alcohol spout contacts triggered photostimulation delivered at increasing intensities over days (10 to 130 mW/mm^2). During recovery sessions, no light was delivered. (**E**) Example alcohol lick event records. (**F**) Area under the light power density curve was lower in ChR2 animals than in eYFP controls (unpaired *t* test, $t_{(12)} = 5.811$, ****p* = 0.0002). (**G**) Area under the light power density curve did not differ between ChR2 animals and eYFP controls (unpaired *t* test, $t_{(12)} = 0.2834$, $p = 0.78$). (**H**) AUC for alcohol licks during recovery sessions was decreased in ChR2 animals compared with eYFP controls (unpaired *t* test, $t_{(12)} = 4.677$, ****p* = 0.0005). (**I**) AUC for licks on the water spout during recovery sessions did not differ between ChR2 animals and eYFP controls (unpaired *t* test, $t_{(12)} = 1.682$, $p = 0.1184$). Error bars indicate ± SEM.

We posit that photoinhibition drives compulsive drinking by disrupting the transmittance of a punishment signal from the mPFC to the dPAG. Whereas this circuit encodes the aversive aspects of stimuli (*24*), it does not appear to be specific to pain, given that quinine functions as a punishment but is not a nociceptive stimulus (Fig. 3).

To determine the behavioral impact of driving excitatory activity in this circuit, we bilaterally expressed channelrhodopsin-2 (ChR2) in mPFC-dPAG neurons and implanted optic fibers over the mPFC (Fig. 4A and fig. S11). The photostimulation-paired side was avoided in a real-time place aversion assay (Fig. 4B) without affecting locomotor activity (Fig. 4C) or anxiety-related behavior (fig. S12).

To test the effects of mPFC-dPAG activation on drinking, we again used a two-bottle choice task in which contacts on either the water or alcohol lickometer triggered photostimulation (Fig. 4D). Alcohol and water remained unadulterated throughout the experiment, and the light power delivered to drive photoexcitation was increased across sessions (10 to 130 mW/mm^2), followed by recovery sessions without photostimulation (Fig. 4E). Photostimulation was sufficient to act as a punishment, producing light-power-dependent decreases in licking for alcohol (Fig. 4F) but not water (Fig. 4G), with lasting decreases in alcohol consumption during recovery (Fig. 4, H and I). Microstructural analysis of licking behavior revealed photostimulation-induced changes in bout structure and timing (fig. S13). Photostimulation produced robust and long-lasting decreases in front-loading behavior (drinking a disproportionate amount of alcohol during the initial portion of the access period), a hallmark measure of addiction-like behaviors (fig. S13, L and N).

In conclusion, we established a behavioral model for multidimensional analysis of drinking behaviors and their evolution across time and with experience. We identified a cortical-brainstem circuit that serves as both a biomarker and a circuit-specific cellular substrate for the development of compulsive drinking.

REFERENCES AND NOTES

1. Substance Abuse and Mental Health Services Administration, Center for Behavioral Health Statistics and Quality, *Results from the 2017 National Survey on Drug Use and Health: Detailed Tables* (2017); www.samhsa.gov/data/sites/default/files/cbhsq-reports/NSDUHDetailedTabs2017/NSDUHDetailedTabs2017.pdf.
2. B. F. Grant, R. B. Goldstein, T. D. Saha, S. P. Chou, J. Jung, H. Zhang, R. P. Pickering, W. J. Ruan, S. M. Smith, B. Huang, D. S. Hasin, *JAMA Psychiatry* **72**, 757–766 (2015).
3. F. W. Hopf, H. M. B. Lesscher, *Alcohol* **48**, 253–264 (2014).
4. L. J. M. J. Vanderschuren, B. J. Everitt, *Science* **305**, 1017–1019 (2004).
5. American Psychiatric Association, *Diagnostic and Statistical Manual of Mental Disorders* (*DSM-5®*) (American Psychiatric Association, 2013).
6. K. McFarland, C. C. Lapish, P. W. Kalivas, *J. Neurosci.* **23**, 3531–3537 (2003).
7. B. T. Chen, H.-J. Yau, C. Hatch, I. Kusumoto-Yoshida, S. L. Cho, F. W. Hopf, A. Bonci, *Nature* **496**, 359–362 (2013).
8. G. F. Koob, N. D. Volkow, *Neuropsychopharmacology* **35**, 217–238 (2010).
9. P. W. Kalivas, N. Volkow, J. Seamans, *Neuron* **45**, 647–650 (2005).
10. J. W. Dalley, B. J. Everitt, T. W. Robbins, *Neuron* **69**, 680–694 (2011).
11. M. M. Silveri, J. Rogowska, A. McCaffrey, D. A. Yurgelun-Todd, *Alcohol. Clin. Exp. Res.* **35**, 218–228 (2011).
12. A. D. Schweinsburg, M. P. Paulus, V. C. Barlett, L. A. Killeen, L. C. Caldwell, C. Pulido, S. A. Brown, S. F. Tapert, *Ann. N. Y. Acad. Sci.* **1021**, 391–394 (2004).
13. O. M. Mahmood, D. Goldenberg, R. Thayer, R. Migliorini, A. N. Simmons, S. F. Tapert, *Addict. Behav.* **38**, 1435–1441 (2013).
14. T. Seif, S.-J. Chang, J. A. Simms, S. L. Gibb, J. Dadgar, B. T. Chen, B. K. Harvey, D. Ron, R. O. Messing, A. Bonci, F. W. Hopf, *Nat. Neurosci.* **16**, 1094–1100 (2013).
15. O. George, C. Sanders, J. Freiling, E. Grigoryan, S. Vu, C. D. Allen, E. Crawford, C. D. Mandyam, G. F. Koob, *Proc. Natl. Acad. Sci. U.S.A.* **109**, 18156–18161 (2012).
16. A. Holmes, P. J. Fitzgerald, K. P. MacPherson, L. DeBrouse, G. Colacicco, S. M. Flynn, S. Masneuf, K. E. Pleil, C. Li, C. A. Marcinkiewcz, T. L. Kash, O. Gunduz-Cinar, M. Camp, *Nat. Neurosci.* **15**, 1359–1361 (2012).
17. K. E. Pleil, E. G. Lowery-Gionta, N. A. Crowley, C. Li, C. A. Marcinkiewcz, J. H. Rose, N. M. McCall, A. M. Maldonado-Devincci, A. L. Morrow, S. R. Jones, T. L. Kash, *Neuropharmacology* **99**, 735–749 (2015).
18. D. M. Lovinger, J. C. Crabbe, *Nat. Neurosci.* **8**, 1471–1480 (2005).
19. C. Giuliano, Y. Peña-Oliver, C. R. Goodlett, R. N. Cardinal, T. W. Robbins, E. T. Bullmore, D. Belin, B. J. Everitt, *Neuropsychopharmacology* **43**, 728–738 (2018).
20. M. Roberto, M. T. Cruz, N. W. Gilpin, V. Sabino, P. Schweitzer, M. Bajo, P. Cottone, S. G. Madamba, D. G. Stouffer, E. P. Zorrilla, G. F. Koob, G. R. Siggins, L. H. Parsons, *Biol. Psychiatry* **67**, 831–839 (2010).
21. K. Goltseker, F. W. Hopf, S. Barak, *Alcohol* **74**, 73–82 (2019).
22. T. E. Thiele, M. Navarro, *Alcohol* **48**, 235–241 (2014).
23. T. B. Franklin, B. A. Silva, Z. Perova, L. Marrone, M. E. Masferrer, Y. Zhan, A. Kaplan, L. Greetham, V. Verrechia, A. Halman, S. Pagella, A. L. Vyssotski, A. Illarionova, V. Grinevich, T. Branco, C. T. Gross, *Nat. Neurosci.* **20**, 260–270 (2017).
24. C. M. Vander Weele, C. A. Siciliano, G. A. Matthews, P. Namburi, E. M. Izadmehr, I. C. Espinel, E. H. Nieh, E. H. S. Schut, N. Padilla-Coreano, A. Burgos-Robles, C.-J. Chang, E. Y. Kimchi, A. Beyeler, R. Wichmann, C. P. Wildes, K. M. Tye, *Nature* **563**, 397–401 (2018).
25. Y. Li, J. Zeng, J. Zhang, C. Yue, W. Zhong, Z. Liu, Q. Feng, M. Luo, *Neuron* **97**, 911–924.e5 (2018).
26. D. A. Evans, A. V. Stempel, R. Vale, S. Ruehle, Y. Lefler, T. Branco, *Nature* **558**, 590–594 (2018).
27. R. R. Rozeske, D. Jercog, N. Karalis, F. Chaudun, S. Khoder, D. Girard, N. Winke, C. Herry, *Neuron* **97**, 898–910.e6 (2018).
28. A. Cabral, N. Isoardi, C. Salum, C. E. Macedo, M. J. Nobre, V. A. Molina, M. L. Brandão, *Exp. Neurol.* **200**, 200–208 (2006).
29. E. M. Avegno, T. D. Lobell, C. A. Itoga, B. B. Baynes, A. M. Whitaker, M. M. Weera, S. Edwards, J. W. Middleton, N. W. Gilpin, *J. Neurosci.* **38**, 7761–7773 (2018).
30. C. A. Siciliano, K. M. Tye, *Alcohol* **74**, 47–63 (2019).
31. E. J. Kremer, S. Boutin, M. Chillon, O. Danos, *J. Virol.* **74**, 505–512 (2000).
32. J. S. Rhodes, K. Best, J. K. Belknap, D. A. Finn, J. C. Crabbe, *Physiol. Behav.* **84**, 53–63 (2005).
33. J. S. Rhodes, M. M. Ford, C.-H. Yu, L. L. Brown, D. A. Finn, T. Garland Jr., J. C. Crabbe, *Genes Brain Behav.* **6**, 1–18 (2007).
34. M. V. Wilcox, V. C. Cuzon Carlson, N. Sherazee, G. M. Sprow, R. Bock, T. E. Thiele, D. M. Lovinger, V. A. Alvarez, *Neuropsychopharmacology* **39**, 579–594 (2014).
35. Y. Ziv, L. D. Burns, E. D. Cocker, E. O. Hamel, K. K. Ghosh, L. J. Kitch, A. El Gamal, M. J. Schnitzer, *Nat. Neurosci.* **16**, 264–266 (2013).
36. K. K. Ghosh, L. D. Burns, E. D. Cocker, A. Nimmerjahn, Y. Ziv, A. E. Gamal, M. J. Schnitzer, *Nat. Methods* **8**, 871–878 (2011).
37. P. Zhou, S. L. Resendez, J. Rodriguez-Romaguera, J. C. Jimenez, S. Q. Neufeld, A. Giovannucci, J. Friedrich, E. A. Pnevmatikakis, G. D. Stuber, R. Hen, M. A. Kheirbek, B. L. Sabatini, R. E. Kass, L. Paninski, *eLife* **7**, e28728 (2018).
38. M. Murugan, H. J. Jang, M. Park, E. M. Miller, J. Cox, J. P. Taliaferro, N. F. Parker, V. Bhave, H. Hur, Y. Liang, A. R. Nectow, J. W. Pillow, I. B. Witten, *Cell* **171**, 1663–1677.e16 (2017).
39. J. M. Otis, V. M. K. Namboodiri, A. M. Matan, E. S. Voets, E. P. Mohorn, O. Kosyk, J. A. McHenry, J. E. Robinson, S. L. Resendez, M. A. Rossi, G. D. Stuber, *Nature* **543**, 103–107 (2017).
40. C.-J. Chang, *Technical Report: Building a Neural Ensemble Decoder by Extracting Features Shared Across Multiple Populations* (MIT, 2019); https://dspace.mit.edu/bitstream/handle/1721.1/122041/Chang-Technical_Report092019.pdf?sequence=1&isAllowed=y.
41. A. M. Stamatakis, G. D. Stuber, *Nat. Neurosci.* **15**, 1105–1107 (2012).
42. A. V. Kravitz, L. D. Tye, A. C. Kreitzer, *Nat. Neurosci.* **15**, 816–818 (2012).
43. J. Olds, P. Milner, *J. Comp. Physiol. Psychol.* **47**, 419–427 (1954).
44. G. D. Stuber, D. R. Sparta, A. M. Stamatakis, W. A. van Leeuwen, J. E. Hardjoprajitno, S. Cho, K. M. Tye, K. A. Kempadoo, F. Zhang, K. Deisseroth, A. Bonci, *Nature* **475**, 377–380 (2011).
45. S. Pellow, P. Chopin, S. E. File, M. Briley, *J. Neurosci. Methods* **14**, 149–167 (1985).

ACKNOWLEDGMENTS

We thank Y.-N. Leow for experimental assistance and C. Wildes and R. Wichmann for technical assistance. **Funding:** C.A.S. was supported by NIH grants F32 MH111216 (NIMH) and K99 DA045103 (NIDA) and a NARSAD Young Investigator Award from the Brain and Behavior Research Foundation. K.M.T. is a New York Stem Cell Foundation–Robertson Investigator and McKnight Scholar and was supported by funding from the JPB Foundation, New York Stem Cell Foundation, R01-MH102441 (NIMH), the NIH Director's New Innovator Award DP2-DK102256 (NIDDK), and Pioneer Award DP1-AT009925 (NCCIH). M.H. was supported by the JPB Foundation. D.L. is enrolled as a student at the Medical Faculty Heidelberg, Heidelberg University, Germany, and was supported by a fellowship from the Boehringer Ingelheim Fonds. **Author contributions:** C.A.S. and K.M.T. jointly conceived of the project and designed the experiments. C.A.S., X.C., and A.R.B. performed stereotaxic surgeries. C.A.S. performed calcium-imaging experiments. C.A.S. and E.Y.K. analyzed the data. C.J.C. performed clustering and machine-learning analyses. C.A.S., H.N., D.L., and X.C. performed and analyzed optogenetic experiments. C.A.S., D.L., C.M.V.W., A.R.B., and X.C. performed histological verifications. C.J.C., H.N., J.J.L., and E.Y.K. provided MATLAB scripts and advice for data analysis. C.M.V.W. and J.W. provided technical training. C.A.S., K.M.T., E.Y.K., C.J.C., H.N., M.H., A.N.V., A.R.B., and C.M.V.W. made additional significant intellectual contributions. C.A.S. and K.M.T. wrote the paper. All authors contributed to the editing of the manuscript. **Competing interests:** The authors declare no competing interests. **Data and materials availability:** All experimental data are available in the main text or the supplementary materials.

SUPPLEMENTARY MATERIALS

science.sciencemag.org/content/366/6468/1008/suppl/DC1
Materials and Methods
Figs. S1 to S13
References (*31*–*50*)

View/request a protocol for this paper from *Bio-protocol*.

21 May 2019; accepted 4 October 2019
10.1126/science.aay1186

A cortical-brainstem circuit predicts and governs compulsive alcohol drinking

Cody A. Siciliano, Habiba Noamany, Chia-Jung Chang, Alex R. Brown, Xinhong Chen, Daniel Leible, Jennifer J. Lee, Joyce Wang, Amanda N. Vernon, Caitlin M. Vander Weele, Eyal Y. Kimchi, Myriam Heiman and Kay M. Tye

Science **366** (6468), 1008-1012.
DOI: 10.1126/science.aay1186

A brain circuit to control alcohol intake

Most people are exposed to alcohol at some point in their lives, but only a small fraction will develop a compulsive drinking disorder. Siciliano *et al.* first established a behavioral measure to assess how predisposition interacts with experience to produce compulsive drinking in a subset of mice (see the Perspective by Nixon and Mangieri). In search of the underlying neurobiological mechanism, they discovered that a discrete circuit between the medial prefrontal cortex and brainstem is central for the development of compulsive drinking. This circuit serves as both a biomarker for the development of compulsive drinking and a driver of its expression. It can bidirectionally control compulsive behavior by mitigating or mimicking punishment signals.

Science, this issue p. 1008; see also p. 947